

## de Haas-van Alphen Effect and Fermi Surface of the Ordered Alloy YZn

J.-P. Jan

*Division of Physics, National Research Council of Canada, Ottawa, Ontario K1A 0R6, Canada*

(Received 20 March 1973)

Observations of the de Haas-van Alphen effect in the ordered alloy  $\beta'$ -YZn ( $\beta'$ -brass, or CsCl structure) reveal the existence of a small spherical pocket of carriers, together with an open sheet. There is at this time no satisfactory theoretical model to explain these results. An augmented-plane-wave (APW) calculation predicts a Fermi surface which is topologically inconsistent with the experimental results. There is some degree of agreement with the nearly-free-electron model, which is however of doubtful validity when yttrium is present. Possible modifications to the APW model are discussed.

### I. INTRODUCTION

The ordered alloy  $\beta'$ -YZn has been the object of several recent studies. Schiltz *et al.*<sup>1</sup> measured the elastic constants of the single crystal, Belakhovsky *et al.*<sup>2</sup> calculated the electronic band structure, and Prevender *et al.*<sup>3</sup> studied the lattice dynamics. The results of de Haas-van Alphen (dHvA) experiments are presented here, and compared with the existing models. A preliminary account has already been given elsewhere.<sup>4</sup>

YZn at the equiatomic composition exhibits the CsCl or  $\beta'$ -brass structure.<sup>5</sup> The electronic structure of a few alloys of this type has been studied both theoretically and experimentally (for bibliography, see Jan and Perrott<sup>6</sup>). The Fermi surface of CuZn, AgZn, or PdIn is a reasonable distortion of the nearly-free-electron model corresponding to three electrons per unit cell, in agreement with band-structure calculations.<sup>7</sup> It is of interest to study alloys of the same structure, but with different numbers of electrons per unit cell; YZn with its five valence electrons is an ideal case.

### II. EXPERIMENTAL PROCEDURE

A single crystal of YZn, with a residual resistance ratio of 60, was kindly supplied by Dr. J. F. Smith of the Ames Laboratory, U. S. Atomic Energy Commission, Iowa State University, and its preparation is described elsewhere.<sup>1</sup> The dHvA effect was measured by the modulation method, in a superconducting solenoid capable of delivering 100 kG. Details of the technique have been published previously.<sup>6</sup>

X-ray diffraction powder diagrams, taken in liquid helium at 4.2 K, confirmed the absence of any phase transformation on cooling, and allowed the determination of the lattice parameter at that temperature,  $a = 3.558 \text{ \AA}$ . This can be compared with  $3.5769 \text{ \AA}$  observed at room temperature by Schiltz *et al.*<sup>1</sup>

### III. EXPERIMENTAL RESULTS

The observed dHvA frequencies  $F$  (in G) have been converted into extremal cross-sectional areas of the Fermi surface  $A$ , expressed in units of  $(2\pi/a)^2$  ( $a$  is the lattice parameter) by means of the formula (Gaussian units)

$$A = (ea^2/hc)F = (3.061 \times 10^{-9})F, \quad (1)$$

and are given in Table I and Fig. 1. Table I also lists cyclotron effective masses. Observations were made in the  $\{100\}$  and  $\{110\}$  planes, and in another plane of the  $\langle 100 \rangle$  zone, at  $22^\circ$  from  $\{100\}$ . There was excellent agreement between different runs and various samples.

The  $\alpha$  branch is independent of crystallographic orientation, within experimental accuracy. This most likely corresponds to a small spherical sheet of Fermi surface, containing  $5.87 \times 10^{-4}$  charge carriers per unit cell. Some evidence of a  $\beta$  branch, with areas fairly independent of orientation and in the range 0.021–0.025, has been reported in preliminary observations,<sup>4</sup> but detailed experiments indicate that it is probably due to the fourth or fifth harmonic of  $\alpha$ , which gives rise to a few oscillations near 100 kG, the field range used for the study of the  $\gamma$  branch.

The  $\gamma$  branch is shown in Fig. 1. The dHvA signals were very weak and difficult to observe, particularly near  $\langle 110 \rangle$ . There is a distinct crossing of branches at  $\langle 110 \rangle$  in the  $\{100\}$  plane, and the short branch near  $\langle 110 \rangle$  in  $\{110\}$  is correspondingly doubly degenerate. This short branch is extremely sensitive to a small misorientation of the crystal; it was necessary to adjust the angular position of the sample very accurately, in order to minimize the beats indicative of a double branch. The results in the plane at  $22^\circ$  from  $\{100\}$  in the  $\langle 100 \rangle$  zone are drawn on two different branches, a fact which will be justified in the discussion. The amplitude of the  $\gamma$  signals vanishes abruptly at the

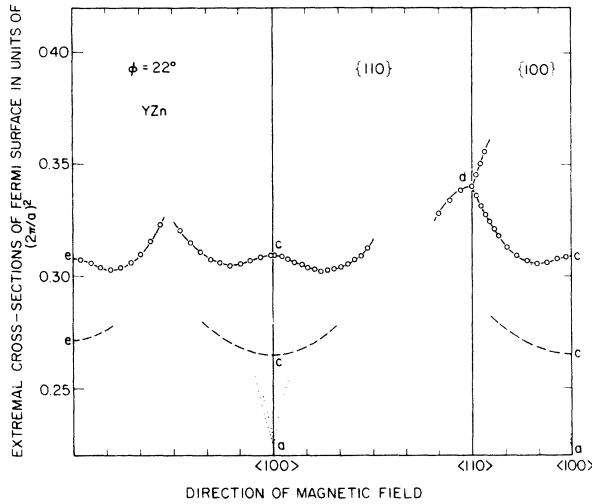


FIG. 1. Experimental results for the  $\gamma$  oscillations (circles, solid lines), and branches of the third band of the NFE model (dashed and dotted lines).

points beyond which they are not observed, and this indicates an open sheet of Fermi surface. This amplitude also goes through a sharp minimum at  $6^\circ$  from  $\langle 110 \rangle$  in  $\{100\}$ . The cyclotron effective masses are large, of the order of two free-electron masses (Table I).

#### IV. DISCUSSION

##### A. Fermi Surface Models

The augmented-plane-wave (APW) band-structure calculation of Belakhovsky, Pierre, and Ray<sup>2</sup> (Fig. 2) allows the determination of a theoretical Fermi surface. The energy bands near the Fermi level are quite far from free-electron bands, due to the  $d$  bands of yttrium (atomic configuration  $4d^1 5s^2$ ); the  $d$  bands of zinc lie far below the Fermi

level. Large effective masses are expected, and indeed observed for the  $\gamma$  branch (Table I). In this APW model, the first band is full, and the second band is almost full, with small hole pockets at  $M$  [cf. Fig. 3(a) for symmetry points]. The third band is an open sheet [Fig. 3(b), Fig. 4] with the topology of arms running along the  $\langle 111 \rangle$  directions, and the next bands are empty. Note that the  $\Lambda_3$  branch lies just below the Fermi level; if it were to cross it, the  $\langle 111 \rangle$  arms in the third band would not exist. Second- and third-band Fermi surfaces are in contact along the cube edge, since the  $T_5$  branch is doubly degenerate. The  $\Lambda_3$  branch is also doubly degenerate, and both degeneracies would be removed by spin-orbit splitting.

As we shall see below, it is of some interest to consider also the nearly-free-electron (NFE) model corresponding to five electrons per unit cell; it is quite different from the APW model. In the first band, it predicts very small hole pockets at  $R$ ; in the second band, slightly larger hole pockets at  $R$ , and a hole closed sheet resembling a cube centered at  $\Gamma$ ; the third band is multiply connected, made of interconnected electron "butterflies" centered at  $M$  (Fig. 4). The fourth band is made of electron "cigars" running along the cube edges and centered at  $M$ .

##### B. $\alpha$ Branch

The spherical symmetry of the small sheet, responsible for the  $\alpha$  oscillations, corresponds to points  $\Gamma$  or  $R$ , which have full cubic symmetry. The small hole pocket at  $M$ , predicted by the APW model, is extremely unlikely to exhibit a spherical shape, since  $M$  has only tetragonal symmetry. A small electron pocket could be obtained, in the fourth band, by lowering slightly point  $R_{1(2^*)}$  (Fig. 2). In the NFE model, the hole pockets at  $R$  in

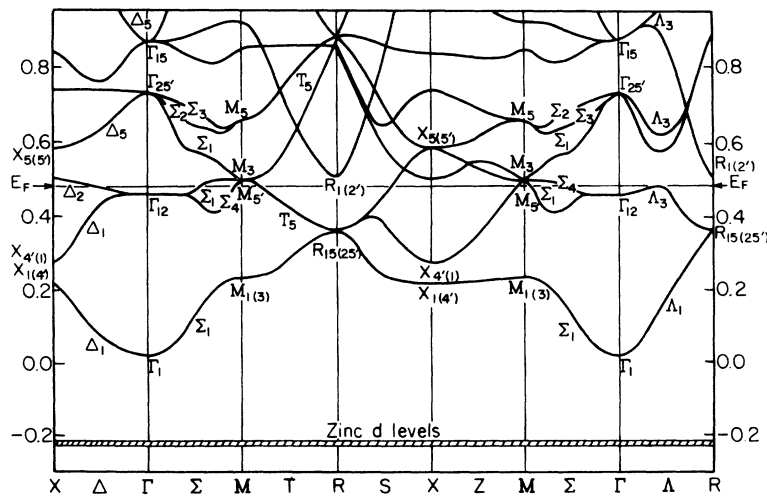


FIG. 2. Theoretical band structure of YZn, after Belakhovsky, Pierre, and Ray (Ref. 2).

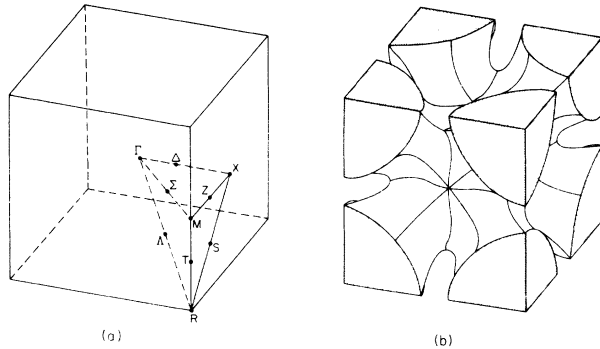


FIG. 3. (a) Brillouin zone and symmetry points for the simple cubic structure. (b) Third band Fermi surface predicted by the APW band-structure calculation of Belakhovsky *et al.*<sup>2</sup>

the first or the second band would have the correct order of magnitude, but would not be expected to exist in the presence of a lattice potential; on the other hand, the closed hole sheet centered at  $\Gamma$  might conceivably shrink to a small sphere, if the model has any validity.

#### C. $\gamma$ Branch

The symmetry of the  $\gamma$  branch is that of an open surface at  $M$  or  $X$ , which both have tetragonal symmetry; in other words, we see only parts of the branches, which are characteristic of a closed sheet centered at  $M$  (or  $X$ ). If we consider ellipsoids of revolution centered at  $M$  ( $X$ ), with their principal axis along  $MR$  ( $XR$ ), and if we match the

cross-sections to those observed at  $\langle 100 \rangle$  and  $\langle 110 \rangle$ , the resulting ellipsoids centered at various points  $M$  ( $X$ ) come into contact, limiting the range of observation of the branches. We get qualitative agreement with the observations, and the volume of these ellipsoids corresponds quite closely to a half-filled zone. The topology is therefore that of intersecting cylinders running along  $MR$  ( $XR$ ).

The symmetry of the  $\gamma$  branch is illustrated in Fig. 5, which is a stereographic plot of the basic triangle for the tetragonal symmetry. The shaded area covers the region in which dHvA signals are observed. The plots confirm that two distinct branches, originating at  $c$  and  $e$ , are seen in the plane at  $22^\circ$ . The double degeneracy of the branch ending at  $a$  in the  $\{110\}$  plane is a further confirmation of the tetragonal symmetry.

The essential feature of the experimental results is a doubly degenerate orbit at  $\langle 110 \rangle$ , one component of which is seen continuously from  $\langle 110 \rangle$  to  $\langle 100 \rangle$  in the  $\{100\}$  plane. Inspection of the APW model shows that it does not predict any branch with this behavior. The APW model does indeed predict a  $\langle 100 \rangle$  orbit of the correct order of magnitude, but it is centered at  $\Gamma$  and therefore does not have the observed symmetry. On the other hand, the APW model predicts a number of orbits which have not been observed, the most obvious one being due to the arms in the  $\langle 111 \rangle$  directions.

Since the APW model appears to be topologically inconsistent with the experimental results, it is tempting to speculate how it could be modified to obtain the correct topology. If we postulate elec-

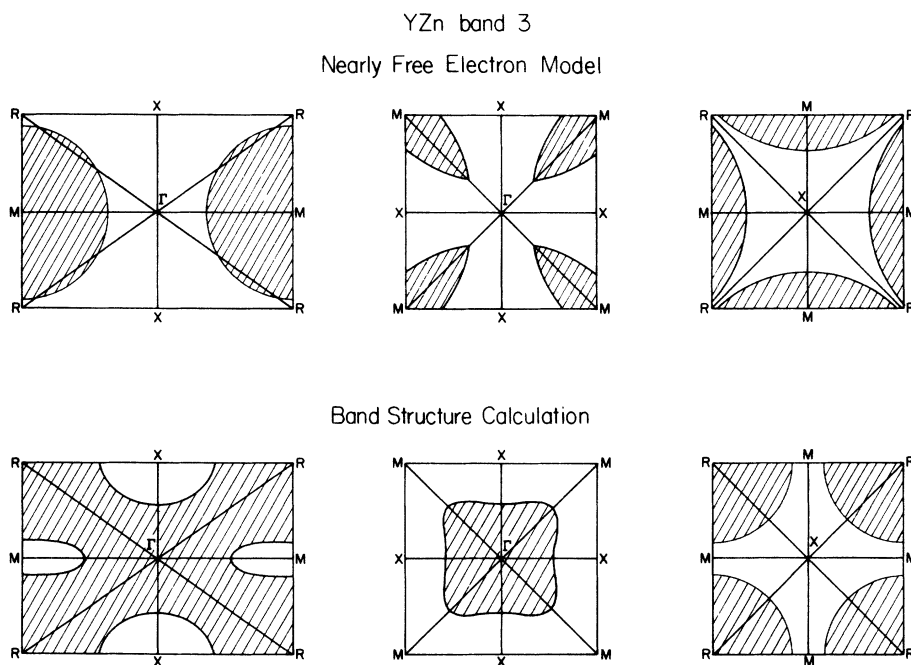


FIG. 4. Comparison between NFE (upper part) and APW (lower part) Fermi surfaces in the third band.

tron cylinders along  $MR$  (or hole cylinders along  $\Gamma X$ ),  $M$  and  $R$  must be occupied,  $\Gamma$  and  $X$  must be empty. This can be achieved by raising  $\Gamma_{12}$  above the Fermi level and lowering  $M_5$  below it. Spin-orbit splitting would remove the degeneracy of  $\Lambda_3$  and  $\Gamma_{12}$  and might help in the right direction; it would also remove the degeneracy of  $M_5$  and  $T_5$ , but the situation there is more complex. Another possibility is that of electron cylinders along  $\Gamma X$  (or hole cylinders along  $MR$ ), which would require lowering  $X$  (unlabeled) below the Fermi level and raising  $R_{15(25^\circ)}$  above it. This last change is very drastic, and is also incompatible with the lowering of  $R_{1(2^\circ)}$  needed to explain the  $\alpha$  branch, leading us to favor the first possibility.

If we now turn to the NFE model we find with some surprise that it appears to explain the  $\gamma$  branch. Its predictions for the third band are shown on Fig. 1. The areas indicated by dashed lines have just the correct magnitude, about 10% lower than the observed branches, and it is not unreasonable that a suitable distortion of the model would extend somewhat their angular range, pushing in particular the  $\{100\}$  branch to  $\langle 110 \rangle$ , where the required crossing point would appear, and beyond. The dotted lines owe their existence to the fact that the "butterflies" do not quite reach the symmetry point  $R$  (Fig. 4), and disappear altogether if  $R$  is an occupied state.

If the NFE model were the only one available, it would have been found adequate, with the following modifications: removal of small hole pockets at  $R$  in the first two bands, reduction of the hole pocket at  $\Gamma$  in the second band to a small sphere, minor modifications of the third band, and removal of the electron pockets in the fourth band. There is some degree of compensation between the removal of holes in the second band and electrons in the fourth band. Agreement with an open sheet of the NFE model, and large orbits, is usually regarded as a good indication of the validity of the model. However, the large effective masses of the  $\gamma$  branch are definitely not free-electron-like.

High-field magnetoresistance would provide valuable information about open orbits, but samples from the same source as ours had a low

TABLE I. Cyclotron effective masses, in units of the free-electron mass, and selected extremal areas, in units of  $(2\pi/a)^2$ .

Magnetic field direction	Frequency branch	Cyclotron effective mass	Extremal area
$\langle 100 \rangle$	$\alpha$	$0.237 \pm 0.001$	$5.341 \times 10^{-3}$
$\langle 100 \rangle$	$\gamma$	$2.08 \pm 0.03$	0.3095
$\langle 110 \rangle$	$\gamma$	$2.36 \pm 0.07$	0.3404
$15^\circ$ from $\langle 100 \rangle$ in $\{100\}$	$\gamma$	$1.99 \pm 0.03$	0.3061

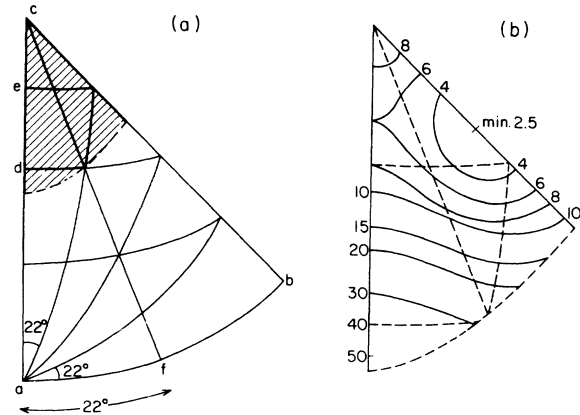


FIG. 5. (a) Stereographic plot, in the basic tetragonal triangle, of the various planes studied; the heavy lines correspond to regions where dHvA signals were observed. The shaded area corresponds to closed extremal orbits. (b) Expanded view of the shaded area of (a), showing contours of equal dHvA frequency; the extremal area, in units of  $(2\pi/a)^2$ , is  $(300+n) \times 10^{-3}$ , where  $n$  is shown in the figure.

residual resistance ratio and were not in the high-field limit at 100 kG.<sup>8</sup>

#### D. Possibility of a Spin-Splitting Zero in the $\gamma$ Branch

The amplitude of the lower  $\gamma$  branch exhibits a sharp dip at an orientation  $6^\circ$  from  $\langle 110 \rangle$  in the  $\{100\}$  plane. A spin-splitting zero arises whenever

$$m^*g = 2n + 1, \quad (2)$$

where  $m^*$  is the cyclotron effective mass, in units of the free-electron mass,  $g$  is the spin-splitting factor, and  $n$  is an integer. If we assume that  $m^*$  varies linearly with the dHvA frequency between  $\langle 110 \rangle$  and the minimum, we get  $m^* = 2.22$  at the amplitude minimum, and the following sequence of possible values for the  $g$  factor: 0.45, 1.35, 2.25, 3.15, etc.

## V. CONCLUSIONS

The experimental results have given evidence of a small spherical sheet of carriers, and of an open surface, the topology of which is consistent with cylinders running along  $MR$  (or  $X\Gamma$ ), but the exact shape of which is not known. The APW model needs only slight modification to explain the first feature, but appears to be topologically incorrect in regard to the open sheet. A modified NFE model can be made consistent with the observations, but this could well be just a coincidence, as the model is not really expected to be valid in the presence of yttrium. The APW model is at any rate in need of serious modifications to bring it in line with the experimental findings. There are strong indications that the introduction of spin-orbit splitting would help in the right direction.

The possibility also exists that a self-consistent calculation would give a better Fermi surface (the calculation of Belakhovsky *et al.*<sup>2</sup> is not self-consistent), or even that the  $4d^1 5s^2$  configuration for *Y* is not adequate as a starting point for the computation of the APW potential.

#### ACKNOWLEDGMENTS

The author is grateful to Dr. J. F. Smith of the Ames Laboratory, U. S. Atomic Energy Commission, Iowa State University, for supplying the

samples; to R. M. Boulet for cutting them; to Dr. J. Pierre for having sent the manuscript of Ref. 2 before its publication, for correspondence, and for kindly supplying sketches of sections of the Fermi surface, which helped in constructing Fig. 3(b); to Dr. A. E. Dunsworth for help with some of the experiments; to N. L. Martin for her assistance with the determination of the lattice parameter, and the calculation and construction of Fermi surface models; and to Dr. I. M. Templeton for reading the manuscript.

- 
- <sup>1</sup>R. J. Schiltz, Jr., T. S. Prevender, and J. F. Smith, *J. Appl. Phys.* **42**, 4680 (1971).  
<sup>2</sup>M. Belakhovsky, J. Pierre, and D. K. Ray, *Phys. Rev. B* **6**, 939 (1972).  
<sup>3</sup>T. S. Prevender, S. K. Sinha, and J. F. Smith, *Phys. Rev. B* **6**, 4438 (1972).  
<sup>4</sup>J.-P. Jan, in *Proceedings of the Thirteenth International Conference on Low-Temperature Physics*, edited by R. H. Kropshot

- and K. D. Timmerhaus (University of Colorado Press, Boulder, Colo., 1972).  
<sup>5</sup>C. C. Chao, H. L. Luo, and P. Duwez, *J. Appl. Phys.* **35**, 257 (1964).  
<sup>6</sup>J.-P. Jan and C. M. Perrott, *J. Low Temp. Phys.* **8**, 195 (1972).  
<sup>7</sup>H. L. Skriver, *Solid State Commun.* **11**, 1355 (1972).  
<sup>8</sup>P. A. Schroeder (private communication).

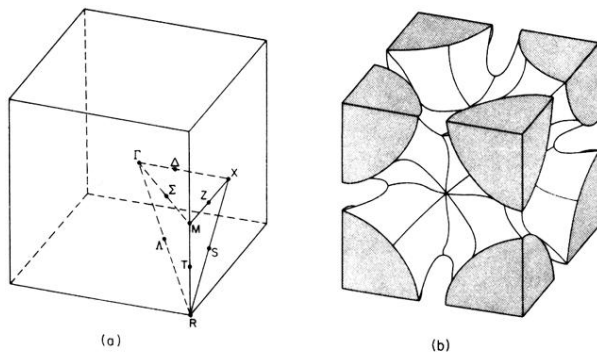


FIG. 3. (a) Brillouin zone and symmetry points for the simple cubic structure. (b) Third band Fermi surface predicted by the APW band-structure calculation of Belakhovsky *et al.*<sup>2</sup>